Mechanical and Trajectory Design of Wearable Supernumerary Robotic Limbs for Crutch Use

by

Michael Yanshun Cheung

Submitted to the
DEPARTMENT OF MECHANICAL ENGINEERING
in Partial Fulfillment of the Requirements for the Degree of

BACHELOR OF SCIENCE IN MECHANICAL ENGINEERING

at the

MASSACHUSETTS INSTITUTE OF TECHNOLOGY

June 2016

Signature of Author: _ Signature redacted
Department of Mechanical Engineering
May 6, 2016

Certified by: ____ Signature redacted
Haruhiko Harry Asada
Professor of Mechanical Engineering
Thesis Supervisor

Accepted by: ___ Signature redacted
Anette Hosoi
Professor of Mechanical Engineering
Undergraduate Officer

Mechanical and Trajectory Design of Wearable Supernumerary Robotic Limbs for Crutch Use

by

Michael Yanshun Cheung

Submitted to the Department of Mechanical Engineering
on May 6, 2016 in Partial Fulfillment of the
Requirements for the Degree of

Bachelor of Science in Mechanical Engineering

ABSTRACT

The Supernumerary Robotic Limbs (SRL) is a wearable robot that augments its user with two robotic limbs, kinematically independent from the user's own limbs. This thesis explores the use of the SRL as a hands-free robotic crutch for assisting injured or elderly people. This paper first details the mechanical and material design choices that drastically reduced the weight of this SRL prototype, including advanced composite materials, efficient joint structure, and high-performance pneumatic actuators. The latter half of this paper characterizes the biomechanics of both traditional crutch-assisted and SRL-assisted ambulation, models this gait pattern with an inverted pendulum system, and derives equations of motion to create a simulation that examines the effect of various initial parameters. Finally, an optimum set of initial parameters is identified to produce a successful SRL-assisted swing.

Thesis Supervisor: Haruhiko Harry Asada
Title: Professor of Mechanical Engineering

Acknowledgements

Special thanks goes to Professor Harry Asada and Ph.D candidate Federico Parietti for their supervision, guidance, and sponsorship in developing this project. Additional thanks to the MIT Hobby Shop and MIT Laboratory for Manufacturing and Productivity for providing manufacturing resources, and MarkForged for providing access to and guidance for their composite 3-D printers.

Table of Contents

List of Figures

1 Introduction

1.1 Wearable Robotics Overview

The field of wearable robots is rapidly expanding and has a wide range of potential applications in augmenting or restoring human movement. Traditional wearable robots are modeled after natural human anatomy and can be broadly classified into *prostheses*, which replace missing body parts; *orthoses*, which provide assistance to impaired patients; and *exoskeletons*, which augment performance of able-bodied users. Exoskeletons and orthoses apply torques in parallel with existing human joints, while prostheses replicate the function and shape of missing body parts [1][2].

Figure 1 Berkeley's BLEEX (Lower Extremity Exoskeleton), designed for carrying heavy loads. This is an example of a conventional exoskeleton where motion is constrained to the natural motion of the user's limbs (in this case, the legs). Image credit Prof. Homayoon Kazerooni.

Conventional exoskeletons designed to work in parallel with human limbs are constrained to the natural motion of the limb (see Figure 1). Additionally, many exoskeletons are designed for a military or emergency-response use case, making them too heavy expensive and heavy for a physical rehabilitation or consumer standpoint [5]. Section 1.2 describes design aspects of the Supernumerary Robotic Limbs that make it more ideal for these use cases.

1.2 Supernumerary Robotic Limbs (SRL) Overview

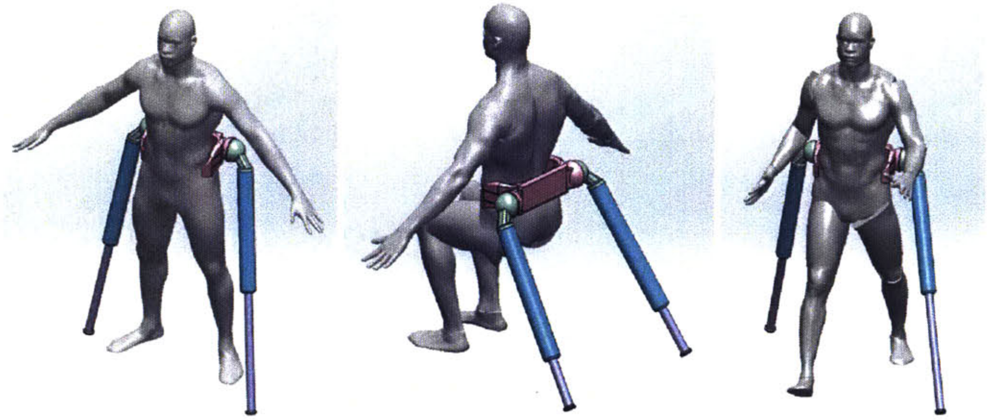

Figure 2 Concept artwork of the SRL, demonstrating different use cases. Left: the robot, worn on a harness around the hip, compensates for user weight while standing. Center: the robot assists the user in the transition from sitting to standing (and vice versa). Right: gait assistance during walking.

The d'Arbeloff Laboratory for Information Systems and Technology at MIT has previously developed prototypes for Supernumerary Robotic Limbs (SRL), a wearable robot that augments a human user with two additional robotic limbs (Figure 2). Unlike conventional exoskeletons, the SRL is not constrained to follow natural limb motions; rather, the robotic limbs are independent from the wearer and can follow optimal control laws [3][4]. This kinematic independence allows for many different complex trajectories and uses. The low mass and volume of the SRL, combined with its trajectory flexibility, differentiate it from other wearable robots. Additionally, the estimated cost of materials for a future product based on this research is on the order of $3000 (which is more than an order of magnitude lower than costs for current state-of-the-art wearable robots).

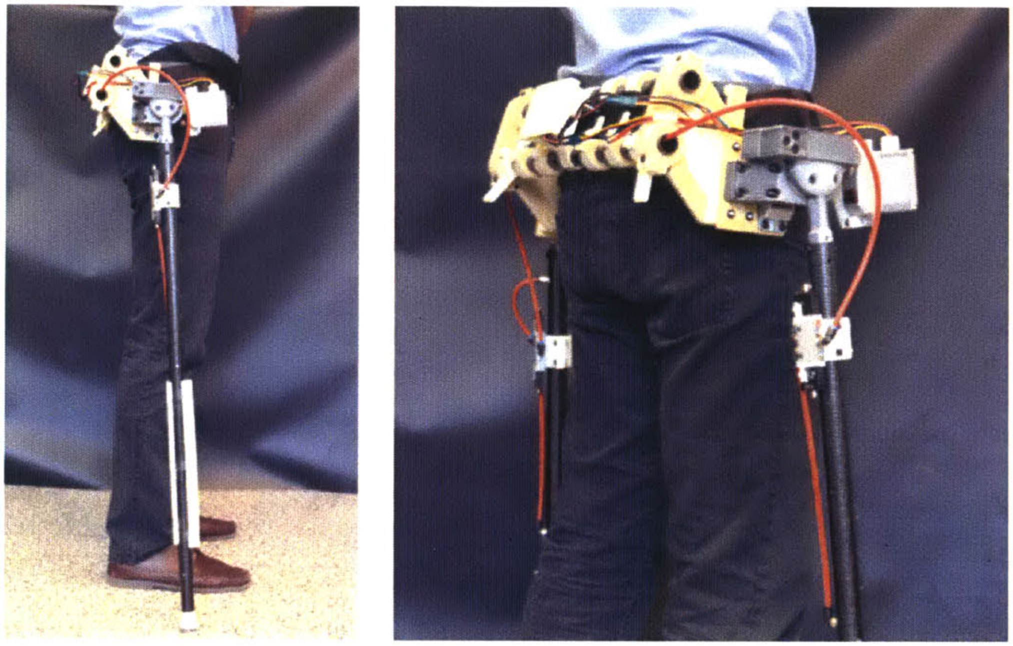

Figure 3 Wearing a prototype of the SRL. The SRL augments a user with two robotic limbs that are kinematically independent from existing limbs. In this prototype, a 3-D printed carbon fiber/Kevlar/nylon composite base, hollow carbon fiber limbs, and lightweight pneumatic cylinders are utilized to reduce overall mass and volume. Image credit Federico Parietti.

Previous work on the SRL in the d'Arbeloff Laboratory has explored several different applications. In a manufacturing context, the SRL can reduce fatigue by compensating for operator weight in uncomfortable positions (like operating on the ceiling or floor), and providing assistance when using heavy powered tools [3]. This weight compensation is achieved through "bracing", where the extra robotic limbs make contact with the environment to provide support for the user. This is a particularly attractive application in the field of manufacturing large, high value products, such as aircraft. Another promising field of application for the SRL is in physical rehabilitation and mobility assistance.

This specific focus of this thesis is on design and optimization of the SRL for the configuration in which it is acting as a pair of active robotic crutches. This use case is of interest because while conventional passive crutches require the use of one or both arms, using the SRL as an active crutch would free the use of both hands. Aside from being beneficial during physical rehabilitation, extra limbs would be useful for mobility assistance of the elderly, for whom loss of balance is a significant risk.

2 Mechanical Design

The SRL is composed of four main parts: a harness, a robotic base containing control electronics and power storage, and two limbs.

Minimizing weight and volume, while maintaining the ability to support the full weight of a user during static and dynamic tasks, were primary design considerations for the SRL. The latest prototype of the SRL, as described in this thesis, achieved a total mass of just 3.5 kg, which is about 4% of the mass of a typical user. This mass is far lower than that of conventional exoskeletons and significantly lower than previous SRL prototypes.

This lightweight performance has been enabled by innovative composite materials and construction methods, joint designs, and actuation choices. These designs are described in more detail in Sections 2.1-2.3.

2.1 Composite materials

All structural load-bearing parts in the latest prototype are 3D printed using Kevlar and carbon fiber, with nylon acting as a fill between the fibers (see Figure 4). This composite structure results in parts with stiffnesses comparable to those of metal parts, with far less weight. This manufacturing process was enabled by a collaboration with MarkForged in Cambridge, MA. These 3D-printed composites contributed to a major weight savings compared to previous SRL prototypes, which used a combination of aluminum and conventional 3D-printed plastic parts.

There are several design considerations unique to MarkForged composite printing that are not present in traditional 3D printing. Fiber orientation strongly influences structural behavior; the MarkForged software allows layer-by-layer patterning of a part, with either concentric patterns or alternating isotropic patterns. Following basic beam theory, because the highest bending stresses develop at the top and bottom surfaces of a beam, structural carbon fiber or Kevlar layers should be placed near the top and bottom surfaces of a part. Other layers can be nylon fill without much penalty to stiffness, which saves cost.

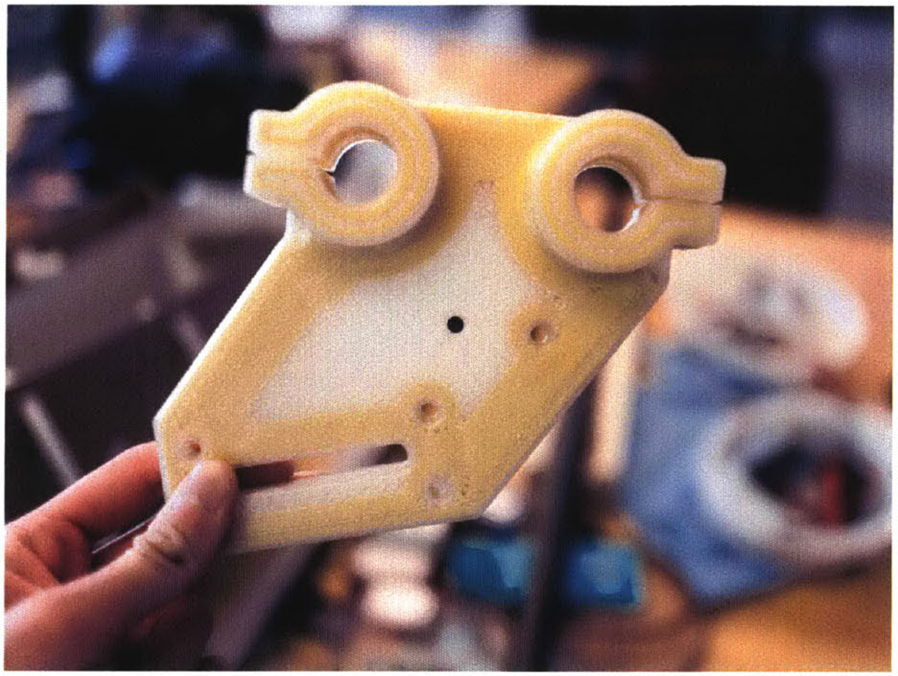

Figure 4 An SRL part printed with Kevlar fiber and nylon fill. The Kevlar fibers are visible in yellow, and are strategically placed around areas experiencing high load.

Additionally, MarkForged's fiber printers are not able to print the same complex overhung/void geometries that traditional 3D-printers can print, necessitating design simplifications in the "hip joint" parts of the SRL base (see Figure 5 for an example of these design simplifications).

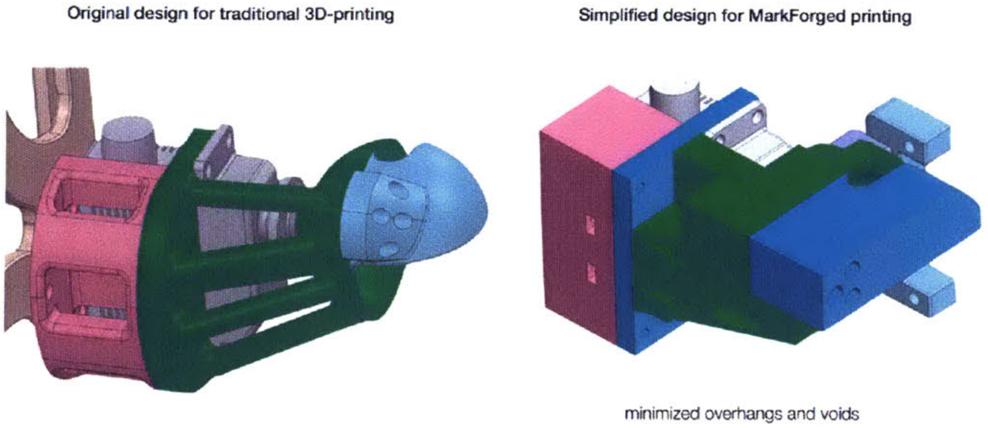
Original design for traditional 3D-printing

Simplified design for MarkForged printing

minimized overhangs and voids

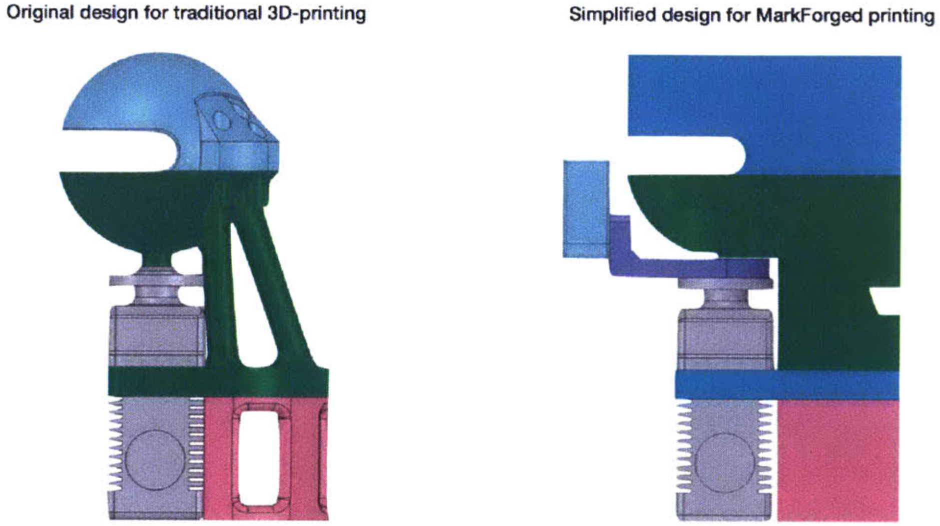
Original design for traditional 3D-printing

Simplified design for MarkForged printing

Figure 5 MarkForged technology allows 3D-printing of carbon fiber and Kevlar parts, but with more geometry constraints than traditional polymer 3D printing.

2.2 Joint design

Each leg of the SRL has two rotational degrees of freedom. These degrees of freedom are combined into a single ball-and-socket joint (Figure 5 and 6). This ball-and-socket, 3-D printed with carbon fiber, absorbs all forces transmitted through the robot leg, eliminating the need for metal shafts or bearings for the two servos that actuate the ball joint.

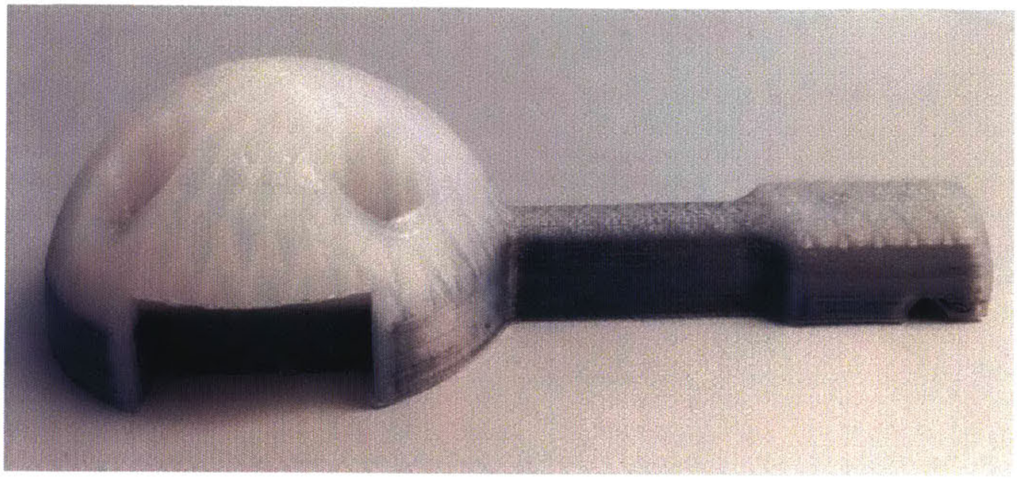

Figure 6 One half of the ball joint. Black layers are printed with carbon fiber; white layers are nylon filler. Ball was printed in two halves due to MarkForged print constraints.

2.3 Linear Actuation and Position Tracking

The linear extension of each limb is actuated by a compact pneumatic cylinder (Figure 7). These actuators are controlled by valves, can produce a maximum force of 500 N, and move fast enough to provide assistance on a wide range of tasks, from weight support to balance support. Each of the compact pneumatic cylinders chosen in this prototype weight less than 1 lb and are cost effective. This represents a large advantage over linear actuators, which are (1) slower because of the high gear ratios needed to generate sufficient forces and (2) heavier because of the metal ball screw transmission needed to support the linear motion.

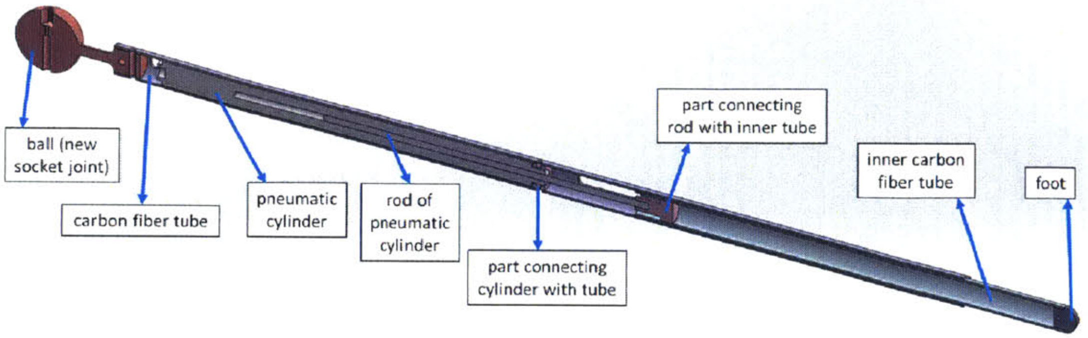

Figure 7 A section view of a limb, showing the inner pneumatic cylinder and simple design architecture. The structure of the leg is a hollow carbon fiber tube, which minimizes mass and inertia.

When designing a system to sense linear extension of the limb, low mass and volume were key constraints. A linear magnetic potentiometer was an ideal solution because it combined low volume with high resolution (well beyond what was needed). Because the wiper does not need to contact the potentiometer, this reduced wear as well. A 3D-printed "shelf" held the magnetic potentiometer in place relative to the outer carbon fiber tube of the limb.

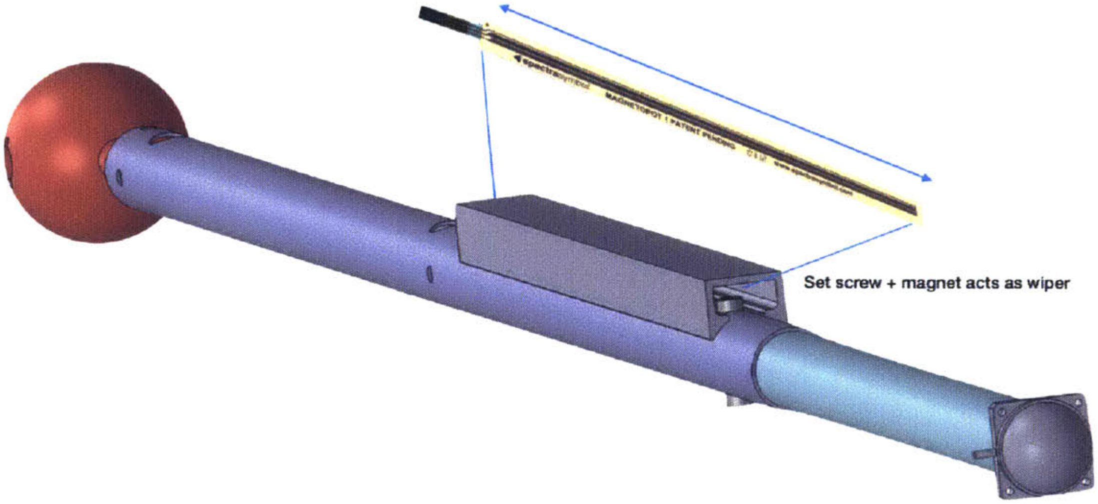

Figure 8 A linear magnetic potentiometer measures linear extension of the leg. The set screw that keeps the inner leg from rotating doubles as the wiper for the potentiometer.

3 Biomechanics of Crutch Use

Ambulation with a crutch can be modeled with a pendulum trajectory. The primary difference between traditional crutch ambulation and SRL-assisted crutch ambulation is the location of the center of mass with relation to the pivot point.

In this thesis's analysis of SRL-crutch ambulation, the limb of the SRL consists of one leg of the pendulum; the ball-and-socket joint of the SRL makes the pivot point. The center of mass for a typical human is approximately 15 cm above the pivot point of the SRL.

Both traditional crutch ambulation and SRL-crutch ambulation are explored in detail in Sections 3.1 and 3.2, respectively. For simplification, all motion will be considered in the sagittal plane since the system is symmetric about the intersection of the sagittal and coronal plane. Figure 9 shows a representation of the anatomical planes.

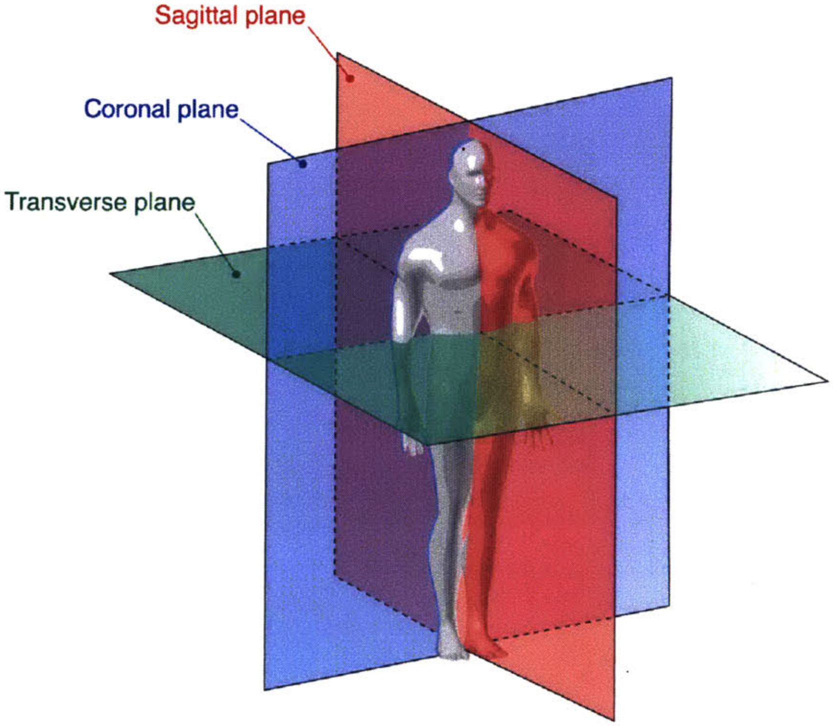

Figure 9 Description of the anatomical planes.

3.1 Traditional Crutch Ambulation

With a traditional crutch, the pivot point about which the person swings is the armpit (where the crutch contacts the body). The crutch serves as one leg of the pendulum, the armpit serves as the pivot point, and the center of mass is below the armpit. This means that the center of mass always remains below the pivot point, making this a pendulum trajectory stable throughout the range of motion. The crutch is assumed not to slip with respect to the floor during the pendulum swing.

Figure 10 is a visualization of this pendulum trajectory. The initial conditions that define trajectory are α_1 , α_2 , τ_1 , τ_2 , $\dot{\alpha_1}$, and $\dot{\alpha_2}$.

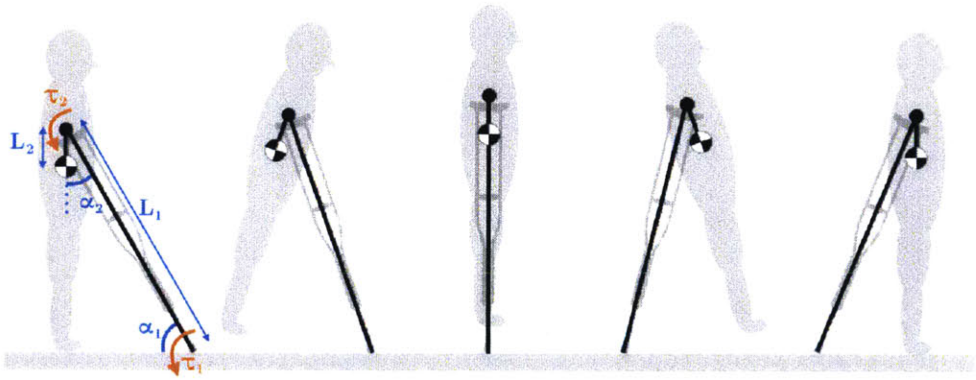

Figure 10 Traditional crutch ambulation can be modeled as a pendulum. The center of mass remains below the pivot point throughout the trajectory.

An Euler-Lagrange analysis results in the following equations of motion:

$$\begin{bmatrix} l_1^2 + l_2^2 + 2l_1l_2\cos(\alpha_2) & l_2^2 + l_1l_2\cos(\alpha_2) \\ l_2^2 + l_1l_2\cos(\alpha_2) & l_2^2 \end{bmatrix} \begin{bmatrix} \ddot{\alpha_1} \\ \ddot{\alpha_2} \end{bmatrix}$$

$$= \begin{bmatrix} 2l_1l_2\sin(\alpha_2)\,\dot{\alpha_1}\dot{\alpha_2} + l_1l_2\sin(\alpha_2)\,\dot{\alpha_2}^2 - gl_1\cos(\alpha_1) - gl_2\cos(\alpha_1+\alpha_2) + \frac{\tau_1}{m} - \frac{\tau_2}{m} \\ l_1l_2\sin(\alpha_2)\,\dot{\alpha_1}\dot{\alpha_2} - l_1l_2\sin(\alpha_2)\,\dot{\alpha_1}^2 - l_1l_2\sin(\alpha_2)\,\dot{\alpha_1}\dot{\alpha_2} - gcos(\alpha_1+\alpha_2) + \frac{\tau_2}{2m} \end{bmatrix}$$

These equations of motion can be linearized about the equilibrium point where $\alpha_1 = \frac{\pi}{2}$ and $\alpha_2 = 0$, resulting in the following:

$$\Delta\ddot{\alpha}_1(l_2^2 - l_1 l_2) + \Delta\ddot{\alpha}_2(l_2^2) + l_1 l_2 \Delta\alpha_2 \Delta\dot{\alpha}_1 \Delta\dot{\alpha}_2 - l_1 l_2 \Delta\alpha_2 (\Delta\dot{\alpha}_1)^2 - l_1 l_2 \Delta\alpha_2 \Delta\dot{\alpha}_1 \Delta\dot{\alpha}_2 + g(\Delta\alpha_1 + \Delta\alpha_2) = \frac{\tau}{2m}$$

3.2 SRL Crutch Ambulation

With the SRL in crutch mode, the pivot point about which the person swings is the ball-and-socket joint of the SRL (which is aligned with the hip). The limb of the SRL consists of one leg of the pendulum; the ball-and-socket joint of the SRL makes the pivot point. The center of mass for a typical human is approximately 15 cm above the pivot point of the SRL. This results in a double inverted pendulum trajectory, which is highly non-linear. This therefore is a more challenging trajectory to control than a traditional crutch trajectory.

During forward motion, the body "vaults" over the robotic limb planted on the ground, raising the center of mass to its highest point as the body passes the vertical, and dropping it back towards the ground. Kinetic energy of forward motion is being converted to a rise in potential energy, until the vertical point is passed at which point the reverse occurs.

Figure 11 is a visualization of this double inverted pendulum trajectory. The initial conditions that define trajectory are α_1 , α_2 , τ_1 , τ_2 , $\dot{\alpha}_1$, and $\dot{\alpha}_2$.

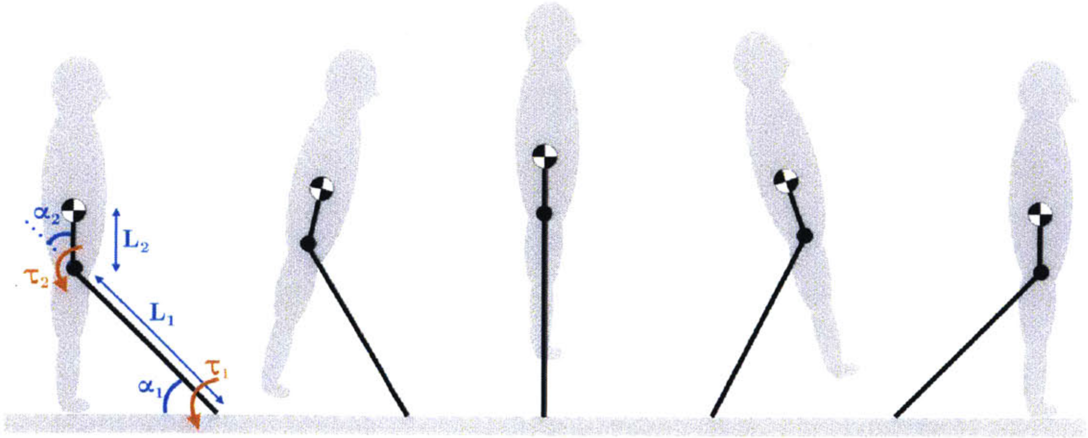

Figure 11 The SRL-crutch trajectory can be modeled as an inverted double pendulum. Note that the center of mass is above the pivot point throughout the swing, making this a highly non-linear system.

As before, an Euler-Lagrange analysis results in the following equations of motion:

$$\begin{bmatrix} l_1^2 + l_2^2 + 2l_1 l_2 \cos(\alpha_2) & l_2^2 + l_1 l_2 \cos(\alpha_2) \\ l_2^2 + l_1 l_2 \cos(\alpha_2) & l_2^2 \end{bmatrix} \begin{bmatrix} \ddot{\alpha}_1 \\ \ddot{\alpha}_2 \end{bmatrix}$$

$$= \begin{bmatrix} 2l_1 l_2 \sin(\alpha_2)\,\dot{\alpha}_1 \dot{\alpha}_2 + l_1 l_2 \sin(\alpha_2)\,\dot{\alpha}_2{}^2 - g l_1 \cos(\alpha_1) - g l_2 \cos(\alpha_1 + \alpha_2) + \frac{\tau_1}{m} - \frac{\tau_2}{m} \\ l_1 l_2 \sin(\alpha_2)\,\dot{\alpha}_1 \dot{\alpha}_2 - l_1 l_2 \sin(\alpha_2)\,\dot{\alpha}_1{}^2 - l_1 l_2 \sin(\alpha_2)\,\dot{\alpha}_1 \dot{\alpha}_2 - g cos(\alpha_1 + \alpha_2) + \frac{\tau_2}{2m} \end{bmatrix}$$

These equations of motion can be linearized about the equilibrium point where $\alpha_1 = \frac{\pi}{2}$ and $\alpha_2 = \pi$, resulting in the following:

$$\Delta\ddot{\alpha}_1(l_2^2 - l_1 l_2) + \Delta\ddot{\alpha}_2(l_2^2) - l_1 l_2 \Delta\alpha_2 \Delta\dot{\alpha}_1 \Delta\dot{\alpha}_2 - l_1 l_2 \Delta\alpha_2 (\Delta\dot{\alpha}_1)^2 - l_1 l_2 \Delta\alpha_2 \Delta\dot{\alpha}_1 \Delta\dot{\alpha}_2 - g(\Delta\alpha_1 + \Delta\alpha_2) = \frac{\tau}{2m}$$

While the linearized equations of motion have the same variables in both the SRL-crutch and traditional crutch cases, note the different signs, indicating how different variables contribute or detract from stability.

4 Trajectory Optimization

Using the equations of motion found in Section 3, we can simulate various trajectories in the SRL-crutch case, varying $\dot{\alpha}_{1,i}$ and $\tau_{2,i}$ to find which combinations result in successful swing completion, defined as when $\alpha_{1,final} = 45^o$ and $\alpha_{2,final} = (45 \pm 15)^o$. Figure 12 is a success matrix showing which initial conditions resulted in success; note the linear region in which success was achieved. The two failure modes were overswing (where the pendulum swung so far, leaving the center of mass at too large of an $\alpha_{2,final}$) and underswing (where the pendulum failed to cross the vertical equilibrium line).

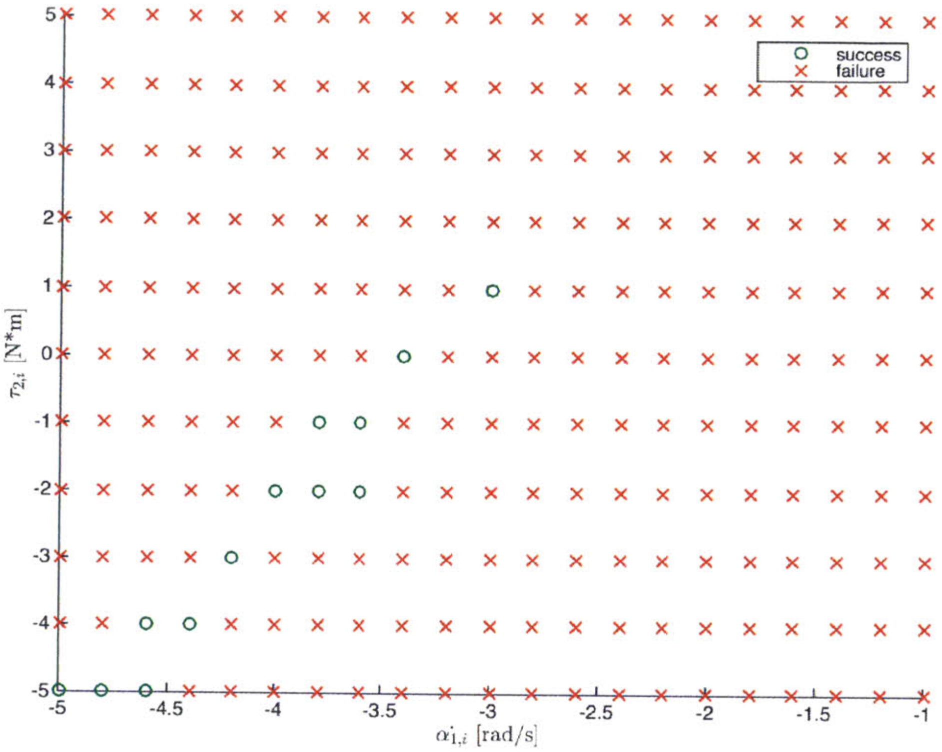

Figure 12 Success matrix, showing simulated trajectory results from various initial values of $\dot{\alpha}_{1,\imath}$ and $\tau_{2,i}$.

To determine which one of these "successful" trajectories was optimal, a cost equation was defined that normalized and summed final $\dot{\alpha}_1$ and final $\dot{\alpha}_2$:

$$Cost = \frac{|\dot{\alpha}_{\iota f}|}{|\alpha\_\{1\dot{m}ax\}|} + \frac{|\dot{\alpha}_{2f}|}{|\alpha\_\{2\dot{m}ax\}|}$$

A lower value of "cost" is better because it minimizes final angular velocities, resulting in a softer landing after the swing trajectory. Figure 13 is a matrix showing values of cost for the "successful" trajectories from Figure 12.

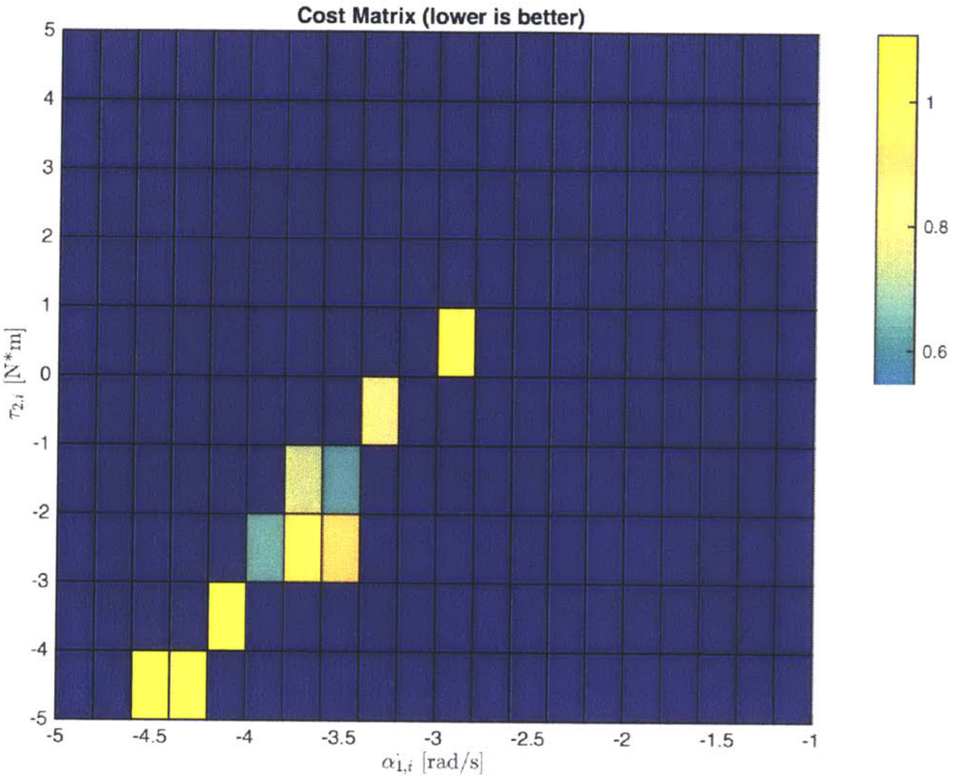

Figure 13 Cost Matrix. The cost equation normalizes and sums final values of final $\dot{\alpha_1}$ and final $\dot{\alpha_2}$.

Based on the Cost matrix (Figure 13), an optimum trajectory was defined, with initial conditions of $\alpha_{1,i} = -3.6\frac{rad}{s}$ and $\tau_{2,i} = -1\frac{N}{m}$. For this optimum trajectory, plots of α_1 , α_2 , $\dot{\alpha_1}$, and $\dot{\alpha_2}$ as well as the final state of the inverted double pendulum are shown in Figure 14.

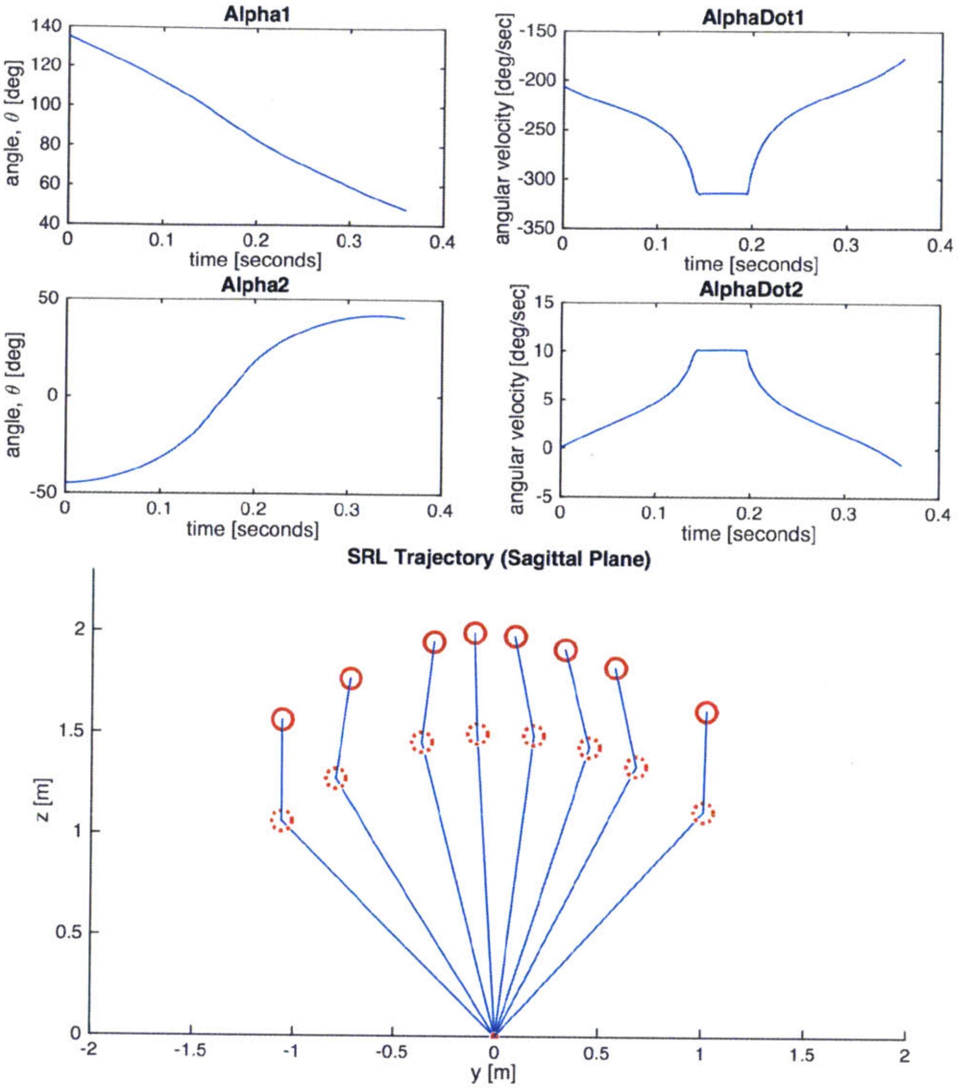

Figure 14 Optimum trajectory, found using methods described in Section 4.

5 Conclusion

The primary goal of this thesis was to explore the use of the SRL as a hands-free robotic crutch for assisting injured or elderly people. Light weight, small volume, and high comfort were requirements to make the SRL a viable choice for this use case.

Innovative mechanical and material design choices were required to drastically reduce the weight of this SRL prototype, including advanced composite materials, efficient joint structure, and high-performance pneumatic actuators. Working with MarkForged's composite 3D printer required design considerations not present in traditional 3D printing.

The biomechanics of both traditional crutch-assisted and SRL-assisted ambulation can be modeled as a pendulum system. The SRL-assisted ambulation case is more challenging because the center of mass remains above the pivot point throughout the swing, resulting in a highly non-linear system. However, simulations identified an optimum set of initial parameters that should produce a successful SRL-assisted swing. Future steps would be to implement this set of initial parameters into real-world testing, and examine how different sized subjects might require different initial parameters.

6 References

1. Bogue, R. (2009). Exoskeletons and robotic prosthetics: a review of recent developments. *Industrial Robot: An International Journal, 36* (5), 421-427.
2. Dollar, A. M., & Herr, H. (2008). Lower extremity exoskeletons and active orthoses: Challenges and state-of-the-art. *Robotics, IEEE Transactions, 24* (1), 144-158.
3. Parietti, F., Asada, H., & Chan, K. (2014, May). Bracing the human body with supernumerary robotic limbs for physical assistance and load reduction. *obotics and Automation (ICRA), 2014 IEEE International Conference*, 14-148.
4. Parietti, F., Chan, K., & Asada, H. (2015, May). Design and control of supernumerary robotic limbs for balance augmentation. *Robotics and Automation (ICRA), 2015 IEEE International Conference*.
5. Zoss, A., & Kazerooni, H. (2006). Design of an electrically actuated lower extremity exoskeleton. *Advanced Robotics*, 967-988.